NASA/TM—2002-211575 ICOMP–2002–02

Airbreathing Pulse Detonation Engine Performance

Louis A. Povinelli
Glenn Research Center, Cleveland, Ohio

Shaye Yungster
Institute for Computational Mechanics in Propulsion, Cleveland, Ohio

May 2002

The NASA STI Program Office . . . in Profile

Since its founding, NASA has been dedicated to the advancement of aeronautics and space science. The NASA Scientific and Technical Information (STI) Program Office plays a key part in helping NASA maintain this important role.

The NASA STI Program Office is operated by Langley Research Center, the Lead Center for NASA's scientific and technical information. The NASA STI Program Office provides access to the NASA STI Database, the largest collection of aeronautical and space science STI in the world. The Program Office is also NASA's institutional mechanism for disseminating the results of its research and development activities. These results are published by NASA in the NASA STI Report Series, which includes the following report types:

- TECHNICAL PUBLICATION. Reports of completed research or a major significant phase of research that present the results of NASA programs and include extensive data or theoretical analysis. Includes compilations of significant scientific and technical data and information deemed to be of continuing reference value. NASA's counterpart of peer-reviewed formal professional papers but has less stringent limitations on manuscript length and extent of graphic presentations.

- TECHNICAL MEMORANDUM. Scientific and technical findings that are preliminary or of specialized interest, e.g., quick release reports, working papers, and bibliographies that contain minimal annotation. Does not contain extensive analysis.

- CONTRACTOR REPORT. Scientific and technical findings by NASA-sponsored contractors and grantees.

- CONFERENCE PUBLICATION. Collected papers from scientific and technical conferences, symposia, seminars, or other meetings sponsored or cosponsored by NASA.

- SPECIAL PUBLICATION. Scientific, technical, or historical information from NASA programs, projects, and missions, often concerned with subjects having substantial public interest.

- TECHNICAL TRANSLATION. English-language translations of foreign scientific and technical material pertinent to NASA's mission.

Specialized services that complement the STI Program Office's diverse offerings include creating custom thesauri, building customized data bases, organizing and publishing research results . . . even providing videos.

For more information about the NASA STI Program Office, see the following:

- Access the NASA STI Program Home Page at ***http://www.sti.nasa.gov***

- E-mail your question via the Internet to help@sti.nasa.gov

- Fax your question to the NASA Access Help Desk at 301–621–0134

- Telephone the NASA Access Help Desk at 301–621–0390

- Write to:
  NASA Access Help Desk
  NASA Center for AeroSpace Information
  7121 Standard Drive
  Hanover, MD 21076

NASA/TM—2002-211575 ICOMP–2002–02

Airbreathing Pulse Detonation Engine Performance

Louis A. Povinelli
Glenn Research Center, Cleveland, Ohio

Shaye Yungster
Institute for Computational Mechanics in Propulsion, Cleveland, Ohio

Prepared for the
Combustion, Airbreathing Propulsion, Propulsion Systems Hazards, and
Modelling and Simulation Subcommittees Joint Meeting
sponsored by the Joint Army-Navy-NASA-Air Force
Destin, Florida, April 8–12, 2002

National Aeronautics and
Space Administration

Glenn Research Center

May 2002

Available from

NASA Center for Aerospace Information
7121 Standard Drive
Hanover, MD 21076

National Technical Information Service
5285 Port Royal Road
Springfield, VA 22100

Available electronically at http://gltrs.grc.nasa.gov/GLTRS

AIRBREATHING PULSE DETONATION ENGINE PERFORMANCE

Louis A. Povinelli*
National Aeronautics and Space Administration
Glenn Research Center
Cleveland, Ohio

Shaye Yungster†
Institute for Computational Mechanics in Propulsion
Cleveland, Ohio

ABSTRACT

This paper presents performance results for pulse detonation engines taking into account the effects of dissociation and recombination. The amount of sensible heat recovered through recombination in the PDE chamber and exhaust process was found to be significant. These results have an impact on the specific thrust, impulse and fuel consumption of the PDE.

INTRODUCTION

In a previous publication (Ref. 1) it was shown that the high temperatures associated with detonation caused a substantial amount of dissociation, yielding high concentrations of intermediate species. This process was accompanied by an 11% decrease in the amount of energy relative to a ramjet available for the production of thrust. The consequence of this loss was to reduce the thermal efficiency of the PDE below the value of the Brayton cycle efficiency at low values of ram air temperature ratios (Ref. 1). Although recombination effects were qualitatively considered, they were not evaluated previously. In this paper, a quantitative evaluation of the effect of recombination was carried out and the amount of sensible heat recovery was determined. In this manner, it may be determined if any significant changes are required to the previous calculations of energy release. The work in references 1 and 2 was based on chemical equilibrium whereas in the present study, finite rate calculations were employed.

PHYSICAL MODEL AND NUMERICAL METHOD

Geometry and Test Gas

Computations were performed for a constant area detonation tube having a length of 1.0 meter and a diameter of 6.6 centimeters. The tube is closed on the left and open on the right. Hydrogen and air having an equivalence ratio, ϕ, of 1.0 and 0.6, with a temperature of 298 K were used as the reactants. Calculations were performed for zero forward flight velocity and at a pressure of 1 bar. At the start of the computation, the entire tube is filled with the hydrogen-air mixture. The ambient pressure outside the detonation tube is set at 1 bar.

To initiate the detonation, we use a small region (2 cm long from the detonation tube head end) of high temperature and high pressure (2500 K and 40 bar) nitrogen gas. In this direct initiation method, the shock wave generated at the interface will transition into a Chapman-Jouguet detonation wave as shown later.

---

* Chief Scientist, Turbomachinery and Propulsion Systems Division.
† Senior Research Associate, Ohio Aerospace Institute.

Computational Method

Finite rate calculations were used to compute the species evolution and resulting thrust and impulse. The analysis was carried out using an in-house developed time-accurate CFD code (Refs. 4, 5). The code solves the axisymmetric Navier-Stokes equations including finite-rate chemistry and real gas effects using an implicit, total variation diminishing (TVD) algorithm. It includes a generalized detailed chemistry capability, various options for turbulence models, and steady-state or time accurate marching algorithms. In the present study, viscous effects were not included, and therefore, the Euler equations were actually used.

The numerical method used for solving the governing equations is described in detail in Ref. 4, and briefly summarized here. The equation set is discretized using a fully implicit, first-order-accurate in time, variable-step backward differentiation formula (BDF) method. The numerical fluxes are discretized using a second-order spatially accurate TVD scheme. The resulting equations are then linearized in a conservative manner and solved iteratively, by using a lower-upper relaxation procedure consisting of successive Gauss-Seidel (LU-SGS) sweeps.

The chemical reaction mechanism for hydrogen-air combustion was based on Jachimowski's model (Ref. 6), and consists of 27 elementary reactions among 12 species. The inversion of large matrices is avoided by partitioning the system into reacting and nonreacting parts. Consequently, the matrices that have to be inverted are of the same size ($N \cdot N$, where N is the number of reacting species) as those that arise in the commonly used point implicit methods. An important advantage of the present method is that, because it is fully implicit, it is stable for large values of the CFL number, thereby enabling the use of relatively large time steps to minimize computational cost.

In order to maintain good resolution of the detonation front at all times, without having to use thousands of grid points, a multi-level, dynamically adaptive grid was implemented in which a very fine subgrid continuously slides along with the detonation wave front (Ref. 7). The minimum and maximum grid spacings used in the present study were 0.00195 cm and 1.0 cm, respectively.

RESULTS

Finite rate chemistry computations were performed for ϕ=1.0 and 0.6. The resulting pressure contours are shown in figure 1 for the stoichiometric case. Figures 1 through 8 show the ϕ=1.0 results. The initial conditions are shown in Fig. 1(a), where the small high pressure zone is observed at the closed end of the tube. At the interface of this region and the combustible mixture, an expansion wave propagates toward the closed end and is reflected from it. Simultaneously, a shock wave moves towards the open end of the tube compressing and heating the hydrogen-air mixture. After a short induction time, combustion begins at the interface boundary sending compression waves upstream and downstream. The compression waves overtake the shock, accelerating it. The shock and combustion front become coupled, forming a detonation wave. Figure 1(b) shows the detonation wave near the end of the tube. The next plots (Figs. 1(c)–(f)) show the detonation expansion process into the surrounding air.

It may be seen that positive pressure is present for approximately 3 milliseconds, during which thrust can occur. The arrival of the rarefaction wave at the head end of the tube can be seen occurring between the last two time sequences.

The computed detonation velocity as a function of time is shown in figure 2, and compared with predictions from the CEA equilibrium code of Gordon and McBride (Ref. 8) for a Chapman-Jouguet detonation. It is observed in figure 2 that after an initial overshoot during the short transient phase, the detonation speed reaches a nearly constant value that is 0.8% higher than that predicted by the CEA code. The corresponding sensible heat release is shown in figure 3 for both the finite rate calculations and the chemical equilibrium results from the CEA code. For comparison, the heat of reaction for hydrogen is also plotted. Note that the CFD results represent the heat released per mass of fuel burnt. It may be seen in figure 3 that the finite rate and equilibrium results differ by 7.5%. The higher heat release for the finite rate calculation is due to chemical recombination inside the tube. Note that both the detonation speed and the heat release are increasing slowly for $t > 0.05$ msec. Therefore, the higher detonation speed computed with the CFD code, as compared with the equilibrium value, could be a result of finite rate chemistry effects.

Figure 4 shows that the passage of the initial detonation pressure spike and temperature rise occurred at 0.5 msec, followed by a rapid decay within 1 msec. The plateau region, where the pressure remains at a level value is seen to persist up to about 3 msec as indicated previously in figure 1. These properties are shown at the exit of the detonation tube.

The changes in gas species are shown in figure 5. The species concentrations are seen to decay rapidly within 2 msec, followed by a slowly decreasing trend. The concentrations of OH, HO2, and H2O2 decline by an order of magnitude, whereas the O and H decline about 2 orders of magnitude in the first 2 msec.

In a second set of computations, the finite rate results were compared with the case where the flow in the tube was frozen when the detonation wave reached the exit of the tube. Figure 6 shows that the temperature profile for the frozen case is approximately 7% lower than that obtained with the finite rate. The species mole fractions at the exit of the tube are shown in figures 7(a)–(c). It is seen that the species concentrations of the finite rate results are lower than those occurring with the frozen flow assumption with the exception of NO.

The corresponding thrust and impulse for the computations described above are shown in figure 8. Initially, the sharp rise in pressure creates a short duration thrust spike (Fig. 8(a)), which is quickly followed by a longer plateau region of 2 msec duration and a subsequent decay to zero. It is primarily during this level pressure duration that PDE thrust is generated. The finite rate profile is slightly greater than that of the frozen case from the range of 1 to 3 msec. The corresponding values of impulse are shown in figure 8(b). The value of the impulse at its maximum point is greater by 5% from the corresponding frozen case.

The PDE results for an equivalence ratio of 0.6 are shown in figures 9 through 12. Figure 9 shows a comparison of the sensible heat release for the finite rate calculation and the chemical equilibrium results for both equivalence ratios. It is noted that the lean equivalence ratio results indicate that the dissociation and recombination processes are less important on their effect on sensible heat release.

Figure 10 shows the temperature profile as observed at the detonation tube exit location. The temperature for both frozen and finite rate chemistry show only a minor difference. A comparison of the intermediate species are shown in figure 11. Generally, the concentrations of the species that contribute to dissociation losses are significantly lower for ϕ=0.6 than those for the stoichiometric results. The corresponding force and impulse behavior are shown in figure 12. In contrast to the ϕ=1.0 results, no substantial differences are present.

The fuel specific impulse was also determined and is shown in figure 13(a) for both equivalence ratios. The specific impulse for ϕ=0.6 was higher than that for ϕ=1.0. However, the thrust for ϕ=0.6 was lower than that at ϕ=1.0 (see figures 12(a) and 8(a)). In figure 13(b), the starting transient that occurs in the first 0.05 msec was neglected. This is justified on the basis of the need to introduce an ignition mechanism to obtain detonation which creates an artificial force that is not representative of the actual initiation process. The specific impulse result based on this correction is shown in figure 13(b). It is observed that the slopes for each equivalence remains unchanged, whereas the maximum values decreased when the ignition transient was neglected. The impulse level also decreased by approximately 10% in the absence of the transient. As in previous results, figure 13(a), the ϕ=0.6 results show greater specific impulse than that for ϕ=1.0.

CONCLUSIONS

The results show that the assumption of frozen flow subsequent to the detonation wave yields lower temperatures at the tube exit for ϕ=1.0; whereas in the case of ϕ=0.6, the differences are negligible. Significant differences were observed in the species mole fractions depending on the equivalence ratio. In general, the rapid decay within the first 2 msec was followed by a more gradual decline for both equivalence ratios. As expected, the absolute level of dissociation was higher for the stoichiometric case. In addition, the force exerted at the head end of the detonation tube shows a small difference, which occurs during most of the process for the ϕ=1.0 case. This force difference was much smaller for the ϕ=0.6 case. The impact on the maximum impulse is of the order of 5.0% for the ϕ=1.0 case, and 2.8% for the ϕ=0.6 case.

The main conclusion drawn from this study was that the dissociation losses occurring during the detonation process for ϕ=1.0 reduces the sensible heat release by approximately 16.7% relative to the heating value, when chemical equilibrium was assumed. Recombination in the PDE reduces this loss to 10.8%. For ϕ=0.6, dissociation effects reduced the sensible heat release by 4.7% (when chemical equilibrium was assumed), and recombination reduces the loss to only 0.6%.

The equivalence ratio comparison indicates that the PDE performance is improved by operation at off-stoichiometric conditions. This suggests operation of a PDE on the lean side provided that sufficient thrust is produced.

REFERENCES

1. Povinelli, Louis A., "Impact of Dissociation and Sensible Heat Release on Pulse Detonation and Gas Turbine Engine Performance," NASA/TM—2001-211080, July 2001, also 15th ISABE Symposium Paper 2001–1212, Sept 2001.

2. Povinelli, L., Lee, J.-H., and Anderberg, M., "Role of Air-Breathing Pulse Detonation Engines in High-Speed Propulsion," NASA/TM—2001-211163, September, 2001, also 52nd International Astronautical Congress Paper IAF-01-S.5.01, Oct 2001.

3. Heiser, William H. and Pratt, David T., "Thermodynamic Cycle Analysis of Pulse Detonation Engines," Jrn. of Propulsion and Power, Vol. 18, No. 1, January-February 2002.

4. Yungster, S. and Radhakrishnan, K., "A Fully Implicit Time Accurate Method for Hypersonic Combustion: Application to Shock-Induced Combustion Instability," *Shock Waves*, Vol. 5, 1996, pp. 293–303.

5. Yungster, S. and Radhakrishnan, K., "Simulation of Unsteady Hypersonic Combustion Around Projectiles in an Expansion Tube," *Shock Waves*, Vol. 11, 2001, pp. 167–177.

6. Jachimowski, C.J., "An Analytical Study of the Hydrogen-Air Reaction Mechanism with Application to Scramjet Combustion," NASA TP–2791, Feb. 1988.

7. Yungster, S. and Radhakrishnan, K., "Computational Study of Near-Limit Propagation of Detonation in Hydrogen-Air Mixtures," to be presented at the 38th AIAA/ASME/SAE/ASEE Joint Propulsion Conference, July 2002, (AIAA paper 2002–3712).

8. Gordon, S. and McBride, B.J., "Computer Program for Calculation of Complex Chemical Equilibrium Compositions and Applications, Part I, Analysis," NASA Reference Publication 1311, October 1994.

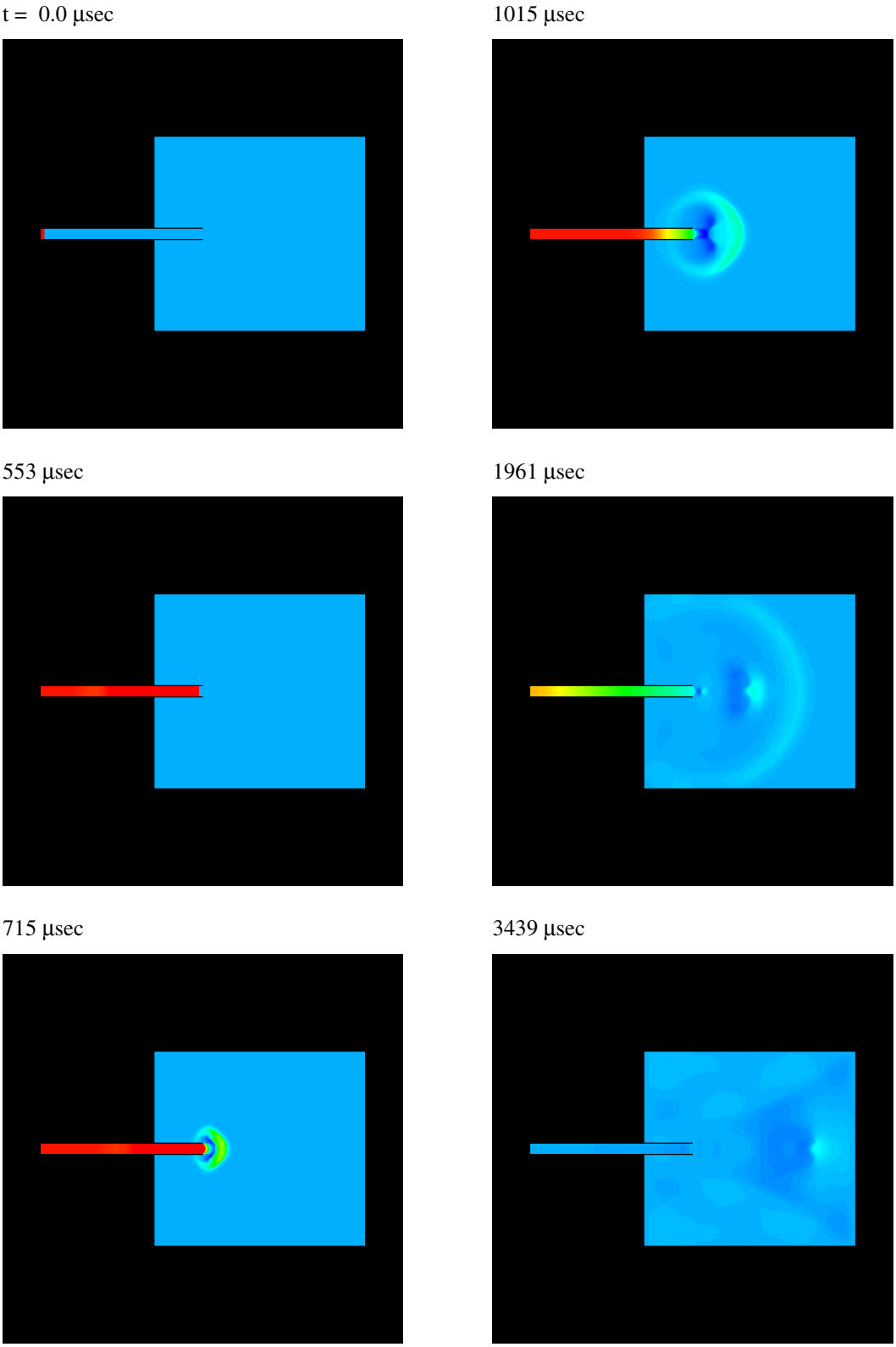

Figure 1. Pressure contours showing temporal evolution of the detonation wave. H_2-air mixture, ϕ=1.0, p_0=1.0 bar, T_o=298 K.

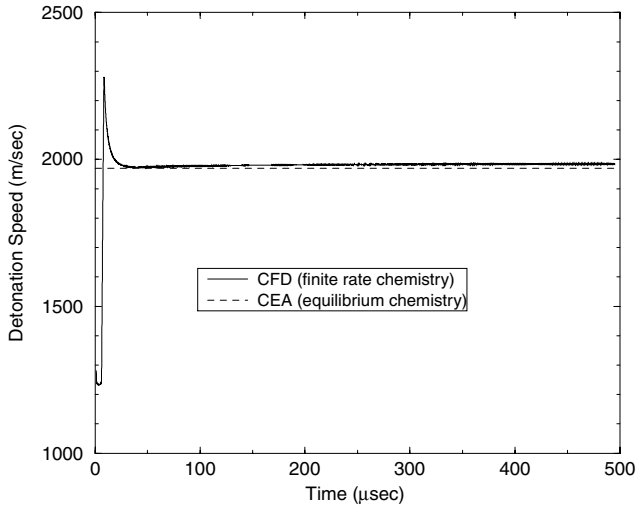

Figure 2. Detonation speed variation with time. H_2-air mixture, ϕ=1.0, p_0=1.0 bar, T_o=298 K.

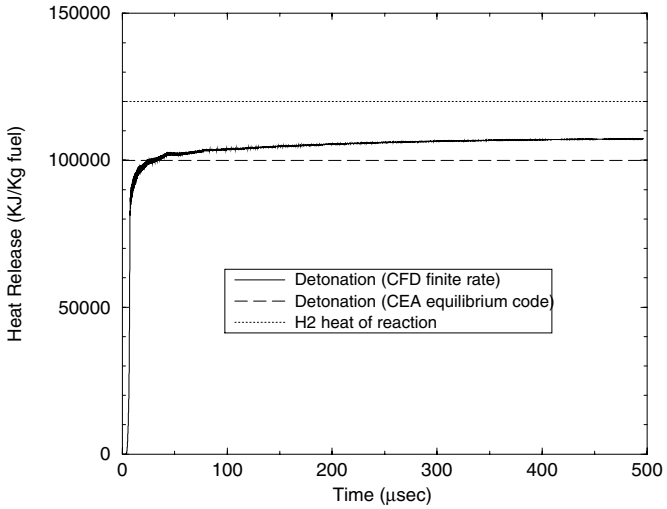

Figure 3. Heat release per mass of burnt fuel as a function of time. H_2-air mixture, ϕ=1.0, p_0=1.0 bar, T_o=298 K.

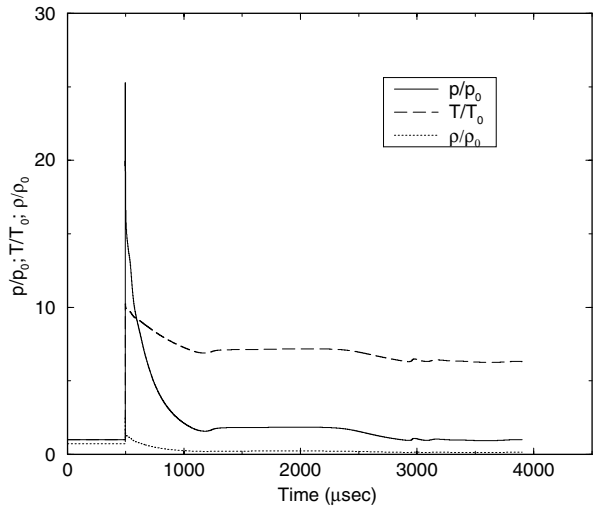

Figure 4. Flowfield conditions at the exit of the detonation tube (x = 1.0 m) as a function of time (ϕ=1.0).

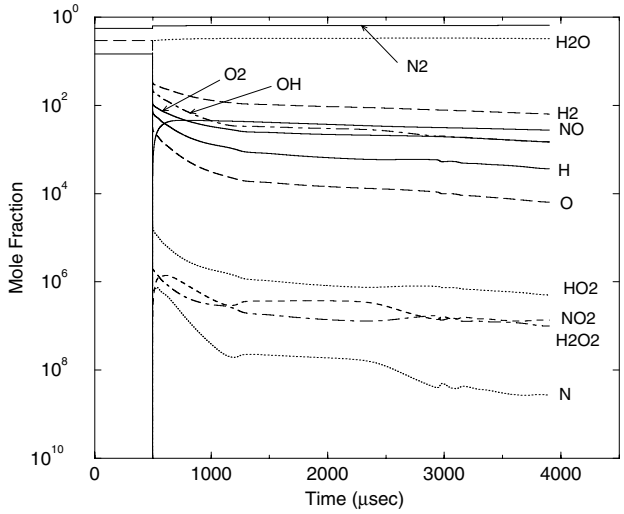

Figure 5. Species mole fractions at the exit of the detonation tube (x = 1.0 m) as a function of time (ϕ=1.0).

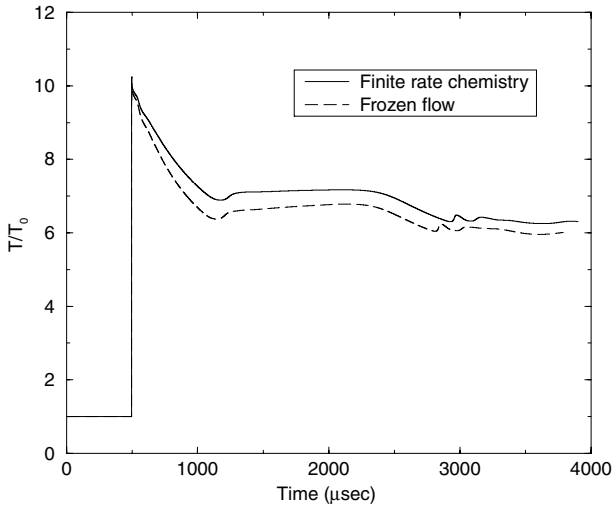

Figure 6. Comparison of temperature at the exit of the detonation tube (x = 1.0 m) between finite rate chemistry flow, and flow that has been frozen after the detonation wave exits the tube (ϕ=1.0).

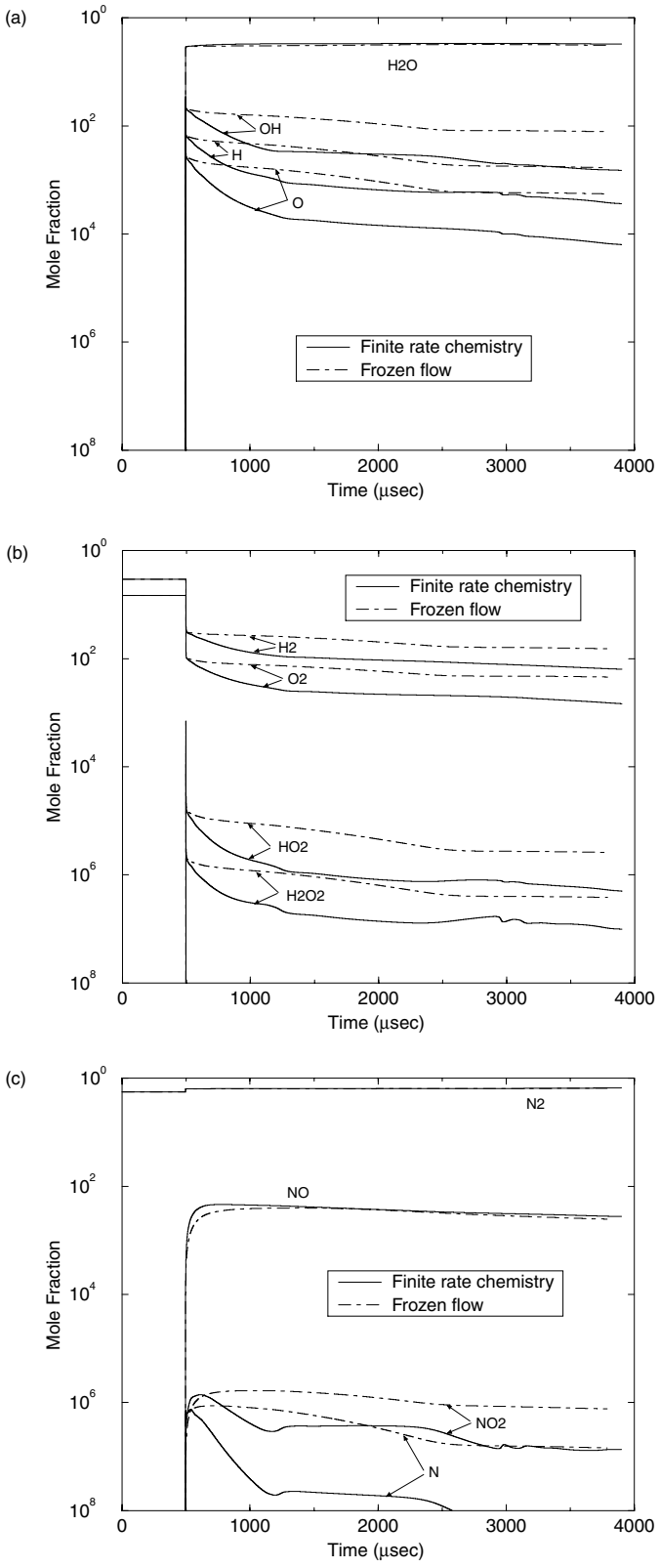

Figure 7. Comparison of species concentration at the exit of the detonation tube (x = 1.0 m) between finite rate chemistry flow, and flow that has been frozen after the detonation wave exits the tube (ϕ=1.0).

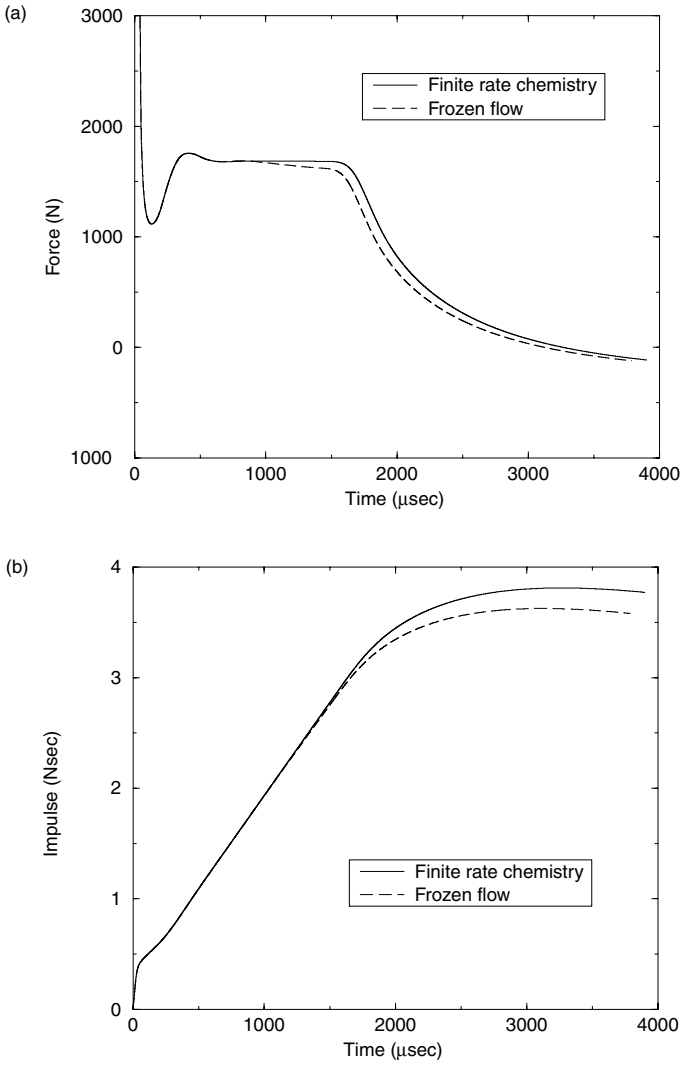

Figure 8. Comparison of force (a) and impulse (b) at the exit of the detonation tube (x = 1.0 m) between finite rate chemistry flow, and flow that has been frozen after the detonation wave exits the tube (ϕ=1.0).

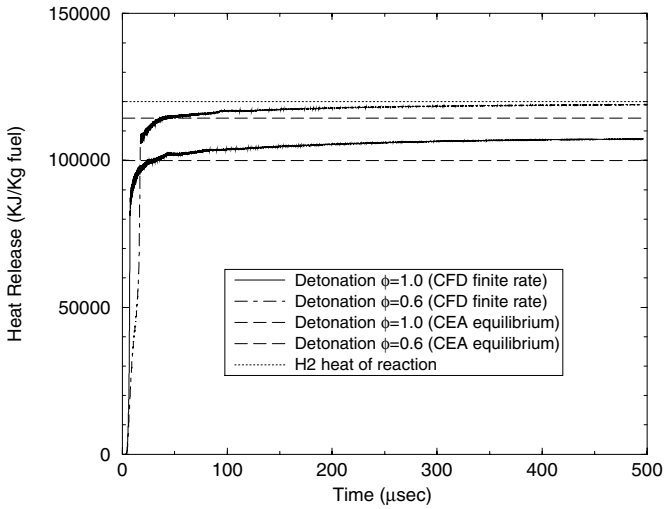

Figure 9. Heat release per mass of burnt fuel as a function of time for the two equivalence ratios.

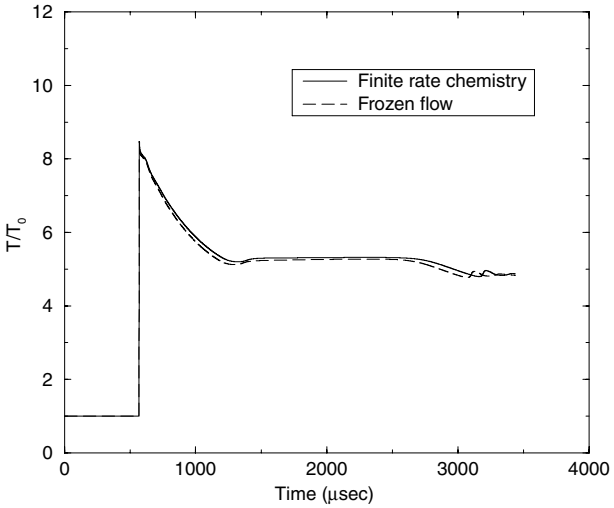

Figure 10. Comparison of temperature at the exit of the detonation tube (x = 1.0 m) between finite rate chemistry flow, and flow that has been frozen after the detonation wave exits the tube (ϕ=0.6).

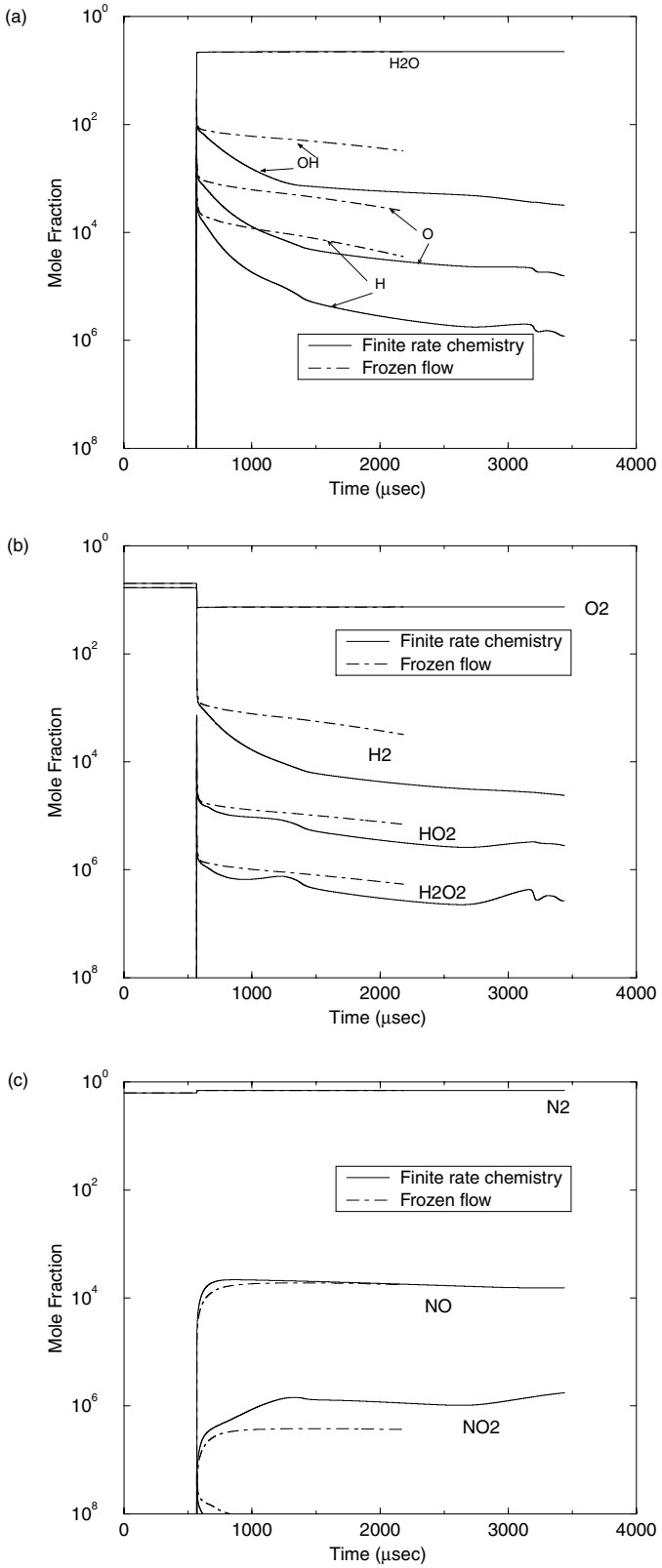

Figure 11. Comparison of species concentration at the exit of the detonation tube (x = 1.0 m) between the finite rate chemistry computations for ϕ=1.0 and ϕ=0.6.

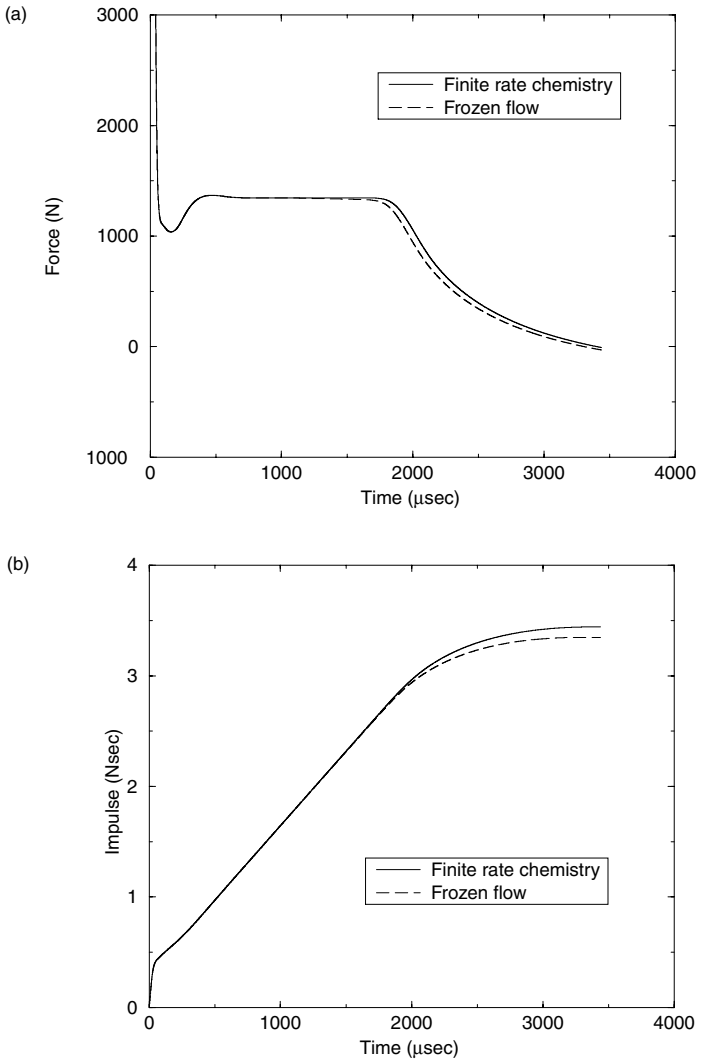

Figure 12. Comparison of force (a) and impulse (b) at the exit of the detonation tube (x = 1.0 m) between finite rate chemistry flow, and flow that has been frozen after the detonation wave exits the tube (ϕ=0.6).

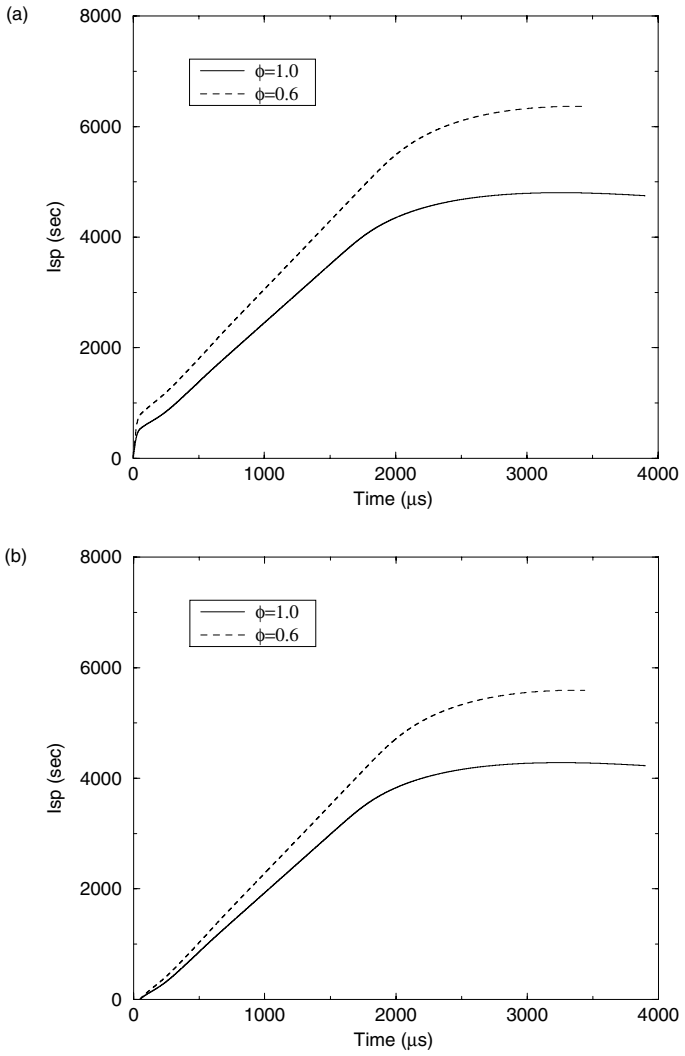

Figure 13. Comparison of specific impulse between the finite rate chemistry computations for ϕ=1.0 and ϕ=0.6. In part (b), the force produced during the starting transient phase (first 50 μsec) was neglected.

REPORT DOCUMENTATION PAGE

Form Approved
OMB No. 0704-0188

1. AGENCY USE ONLY (*Leave blank*)	2. REPORT DATE	3. REPORT TYPE AND DATES COVERED
	May 2002	Technical Memorandum

4. TITLE AND SUBTITLE

Airbreathing Pulse Detonation Engine Performance

5. FUNDING NUMBERS

WU–706–21–33–00

6. AUTHOR(S)

Louis A. Povinelli and Shaye Yungster

7. PERFORMING ORGANIZATION NAME(S) AND ADDRESS(ES)

National Aeronautics and Space Administration
John H. Glenn Research Center at Lewis Field
Cleveland, Ohio 44135–3191

8. PERFORMING ORGANIZATION REPORT NUMBER

E–13359

9. SPONSORING/MONITORING AGENCY NAME(S) AND ADDRESS(ES)

National Aeronautics and Space Administration
Washington, DC 20546–0001

10. SPONSORING/MONITORING AGENCY REPORT NUMBER

NASA TM—2002-211575
ICOMP–2002–02

11. SUPPLEMENTARY NOTES

Prepared for the Combustion, Airbreathing Propulsion, Propulsion Systems Hazards, and Modelling and Simulation Subcommittees Joint Meeting sponsored by the Joint Army-Navy-NASA-Air Force, Destin, Florida, April 8–12, 2002. Louis A. Povinelli, NASA Glenn Research Center, and Shaye Yungster, Institute for Computational Mechanics in Propulsion, Cleveland, Ohio. Responsible person, Louis A. Povinelli, organization code 5000, 216–433–5818.

12a. DISTRIBUTION/AVAILABILITY STATEMENT

Unclassified - Unlimited
Subject Category: 07 Distribution: Nonstandard

Available electronically at http://gltrs.grc.nasa.gov/GLTRS

This publication is available from the NASA Center for AeroSpace Information, 301–621–0390.

12b. DISTRIBUTION CODE

13. ABSTRACT ***(Maximum 200 words)***

This paper presents performance results for pulse detonation engines taking into account the effects of dissociation and recombination. The amount of sensible heat recovered through recombination in the PDE chamber and exhaust process was found to be significant. These results have an impact on the specific thrust, impulse and fuel consumption of the PDE.

14. SUBJECT TERMS

Pulse detonation engines; Airbreathing propulsion; Dissociation and recombination in pulse engines

15. NUMBER OF PAGES

20

16. PRICE CODE

17. SECURITY CLASSIFICATION OF REPORT	18. SECURITY CLASSIFICATION OF THIS PAGE	19. SECURITY CLASSIFICATION OF ABSTRACT	20. LIMITATION OF ABSTRACT
Unclassified	Unclassified	Unclassified	